Photocatalytic degradation of boscalid in aqueous titanium dioxide suspension: Identification of intermediates and degradation pathways

Laura Lagunas-Allué [a,c], María-Teresa Martínez-Soria [a], Jesús Sanz-Asensio [a], Arnaud Salvador [b], Corinne Ferronato [c], Jean Marc Chovelon [c,*]

[a] Department of Chemistry, University of La Rioja, Madre de Dios, 51, 26006 Logroño, Spain
[b] Université Lyon 1, CNRS, UMR 5180, Laboratoire des sciences Analytiques, Batiment CPE 43, Boulevard du 11 novembre 1918, Université de Lyon, 69622 Villeurbanne cedex, France
[c] Université Lyon 1, CNRS, UMR 5256, IRCELYON Institut de recherches sur la catalyse et l'environnement de Lyon (IRCELYON), 2 Avenue Albert Einstein, F-69626 Villeurbanne, France

ARTICLE INFO

ABSTRACT

The photocatalytic degradation of boscalid in aqueous suspensions was investigated by using titanium dioxide (TiO$_2$) as a photocatalyst. Accordingly, a complete degradation of fungicide was achieved by applying the optimal operational conditions of 2.5 g L^{-1} of catalyst, natural pH of 6.0 and the temperature at 20 ± 1 °C after 90 min irradiation. Photodegradation of boscalid exhibited pseudo-first-order reaction kinetics. The rate of photodecomposition of boscalid was measured using high performance liquid chromatography-diode array detector (HPLC-DAD) while its mineralization was followed using total organic carbon (TOC) analysis. The influence of physicochemical parameters such as photonic flux, presence of inorganic cations and anions, pH and oxygen concentration on the kinetic process was studied. The identification of reaction intermediate products was carried out using coupled techniques HPLC–MS/MS after a SPE pre-concentration step and a degradation pathway was proposed. By this technique, 17 degradation products were identified.

© 2010 Elsevier B.V. All rights reserved.

1. Introduction

Grapes are an important crop in Spain and worldwide. High relative humidity and rains favour fungal grapevine diseases which are generally fought using high amounts of different pesticides. A proportion of pesticides inevitably enters the soil and reaches to surface water [1–4] through spraydrift and runoff of soil and suspended sediments. Thus, it could result in a contamination of surface and ground waters, which in turn becomes a potential risk for the environment.

Boscalid [2-chloro-N(4′-chloro-biphenyl-2-yl)-nicotinamide] is a completely new active ingredient belonging to the anilid group of fungicides via a completely novel mode of action recommended for the prevention and treatment of the grey mold (*Botrytis cinerea*) in fruit plants and vines. Its chemical structure is shown in Fig. 1. Boscalid is persistent and by this, it is important to use treatment methods for the removal of this pollutant from water.

There are several methods of removing pesticides from water as microbial degradation, mechanochemical destruction and thermal degradation [5–7]. Although these mentioned methods were available to degrade pesticides, they possessed some limitations such as time-consuming or high manipulation cost. During the past years, some considerations have been focused on the photocatalytic process based on TiO$_2$ [8–10].

Titanium dioxide (TiO$_2$)-based photocatalytic oxidation is a promising technology in water and wastewater treatment because TiO$_2$ is a cheap, stable, operates in ambient temperature and pressure with low energy photons ($\lambda < 388$ nm), requires no chemical reagents except oxygen in the ambient air and is nontoxic catalyst [11–13]. The TiO$_2$-mediated photocatalysis process has been successfully used to degrade pollutants during the past few years [14–18]. The initial step in TiO$_2$-mediated photocatalysis degradation is proposed to involve the generation of an (e$^-$/h$^+$) pair, leading mainly to the formation of hydroxyl radicals (OH$^\bullet$) as well as superoxide radical anions (O$_2^{\bullet-}$) and hydroperoxyl radicals (HOO$^\bullet$) which are able to destroy a large variety of toxic organic compounds [19,20]. Among them, hydroxyl radicals are the most powerful oxidizing species that TiO$_2$ photocatalysis produces.

At present, no studies on the removal of boscalid have been reported and a detailed study of the photocatalytic degradation might provide useful information for the use of TiO$_2$ in the treatment of boscalid in aqueous solution. The aim of this paper is to assess the effectiveness of the photocatalytic process for the decontamination of water polluted by boscalid.

* Corresponding author. Tel.: +33 472 43 26 38; fax: +33 472 44 81 14.
  E-mail addresses: jean-marc.chovelon@univ-lyon1.fr,
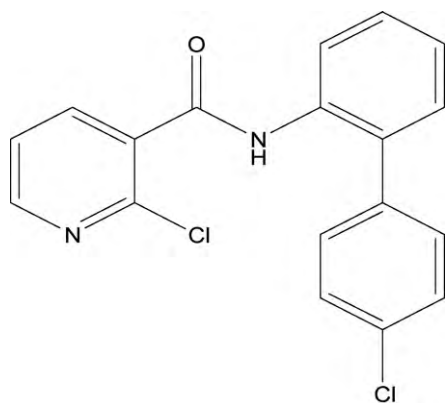chovelon@univ-lyon1.fr (J.M. Chovelon).

Fig. 1. Chemical structure of boscalid.

Thus, the objectives of the study were (a) to evaluate the kinetics aspects of the process (adsorption, degradation rate, photolysis, etc.) and the influence of various parameters such as pH, photonic flux, oxygen concentration and co-existing substances that may affect the photodegradation of boscalid in the presence of TiO_2 suspensions, (b) the identification of the reaction intermediates as well as carboxylic acids and their kinetic evolution profiles during the process of boscalid photodegradation for understanding of the mechanistic details of the photodegradation in the TiO_2/UV light process and (c) monitoring the total organic carbon (TOC).

2. Experimental

2.1. Materials and reagents

Boscalid was purchased from Riedel-de-Haën (Seelze, Germany). Standard solutions containing $3.5 \, mg \, L^{-1}$ of boscalid in water were prepared and protected from light. Non-porous titanium dioxide (TiO_2, P25, Degussa AG, Germany) with primary particle diameter of 30 nm and specific surface area of ca. $50 \, m^2 \, g^{-1}$ was used as the photocatalyst. The solvents used for HPLC analyses were methanol and acetonitrile, HPLC grade from SDS Carlo Erba (Peypin, France) and water was obtained from a Millipore Waters Milli-Q water purification system (Milli-Q-50 18 MΩ). Polyvinylidene fluoride (PVDF) filters ($0.45 \, \mu m$) were purchased from Millipore (Molsheim, France). Formic acid (MS grade, 99% purity) was from Aldrich. Other reagents were at least of analytical grade.

2.2. Photoreactor and light source

The irradiation experiments were carried out in an open Pyrex glass cell of ca. 60 mL containing the aqueous suspension of boscalid and TiO_2 powder. UV-irradiation was provided by a mercury lamp (Philips HPK 125 W) emitting in the near-UV (mainly around 365 nm) cooled with a water circulation and filtered with a 340 nm cut-off filter made of Pyrex. To adjust the intensity of the light source, various types of mesh screen made of stainless steel were adapted between the lamp and the reactor. The actual light flux entering the reactor was measured directly using a radiometer (Bioblock, Illkirch, France Scientific model CX-365). For all experiments, the suspensions were magnetically stirred and the concentration of TiO_2 was $2.5 \, g \, L^{-1}$.

2.3. Procedure

A volume of 25 mL of a solution of boscalid ($3.5 \, mg \, L^{-1}$ or $10.3 \, \mu mol \, L^{-1}$) and 62.5 mg of TiO_2 were introduced in the reactor and vigorously stirred. The solution was allowed to stay in the dark during 15 min to reach adsorption equilibrium and then, it was irradiated. During kinetic experiments, $300 \, \mu L$ aliquots were sampled during adsorption and at different irradiation times and filtered through $0.45 \, \mu m$ PVDF Millipore filters to remove TiO_2 particles before analyses.

All the experiments were performed at a natural pH ≈ 6, with the reactor opened to air and the temperature was initially fixed at $20 \pm 1 \, °C$ and controlled throughout the experiment. During the photocatalytical degradation of boscalid, the pH was measured and only a slight decrease was observed.

2.4. Solid-phase extraction

Before separating and identifying the intermediates formed during the boscalid degradation, the filtered suspensions were concentrated by solid-phase extraction (SPE) method. A sample volume of 25 mL was passed through the Isolute C_{18} cartridges 500 mg/6 mL (International Sorbent Technology, Cambridge, UK), previously conditioned with 6 mL of methanol followed by 6 mL of water using a Varian vacuum manifold. Then, the retained compounds were eluted with two aliquots of 0.5 mL methanol.

2.5. Analytical determination

2.5.1. HPLC-UV and HPLC-DAD analyses
The primary degradation of boscalid was followed by HPLC-DAD (high pressure liquid chromatography-diode array detector; Shimadzu LC-10AT binary pump and SPD-M10A DAD). The analytical column used was an YP5 B C_{18} (125 mm × 4 mm). The flow rate was $1.0 \, mL \, min^{-1}$ and the injection volume was $20 \, \mu L$. The isocratic elution conditions were methanol/water (60:40, v/v); wavelength, 210 nm.

The detection of carboxylic acids was performed using the HPLC-UV system (Varian 9010 model) with a COREGEL 87-H3 cation exchange column ($9 \, \mu m$, 300 mm × 7.8 mm). The mobile phase was H_2SO_4 (pH = 2.0) at a flow rate of $0.6 \, mL \, min^{-1}$. The injection volume was $100 \, \mu L$. The wavelength for detection was 210 nm.

2.5.2. TOC measurements
Total organic carbon (TOC) determinations were carried out using a TOC analyzer BIORITECH model 700 on the filtered irradiated samples of boscalid ($3.5 \, mg \, L^{-1}$).

2.5.3. HPLC–MS/MS analysis
The identification of intermediates was performed by HPLC–MS/MS. In order to detect and identify the maximum number of degradation products, a SPE concentration of 25 mL irradiated solution was performed. Then, a $20 \, \mu L$ sample was injected. LC–MS analyses were performed on a system consisting of an HP 1100 series HPLC instrument comprising a binary pump and autosampler (Agilent Technologies, Waldbronn, Germany) coupled to a API3000 triple quadrupole mass spectrometer (Applied Biosystems/MDS Analytical Technologies, Foster City, CA, USA) equipped with a Turbo IonSpray source. The LC separation was carried out on a Prontosil C_{18} column (125 mm × 2 mm, $3 \, \mu m$) from Atlantic Labo I.C.S (Bruges, France). Elution was performed at a flow rate of $300 \, \mu L \, min^{-1}$ with water containing 0.1% (v/v) formic acid as eluent A and acetonitrile containing 0.1% (v/v) formic acid as eluent B, employing a linear gradient from 10% B to 100% B in 25 min. MS analysis was carried out mainly in negative ionization mode using an ion spray voltage of $-4200 \, V$. Instrument control, data acquisition and processing were performed using the associated Analyst 1.4.2 software. The mass spectrometer was initially calibrated using polypropylene glycol (Applied Biosystems, Foster City, CA, USA). Q1 and Q3 were adjusted to 0.7 ± 0.1 a.m.u.

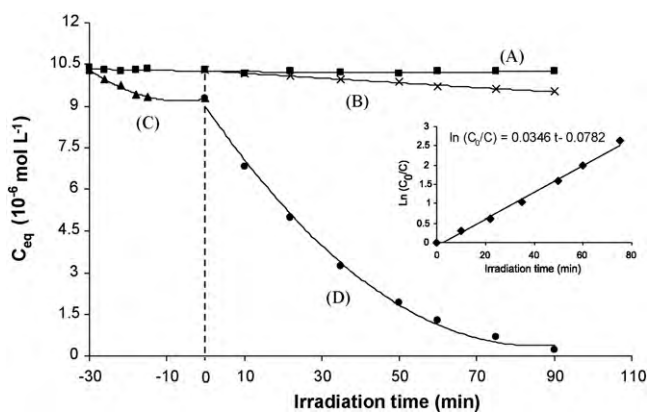**Fig. 2.** Hydrolysis (A), direct photolysis (B), adsorption (C) and photocatalytic degradation (D) of boscalid (10.3 μmol L^{-1}). The inset shows the linear transform of the integrated first-order kinetics.

FWHM for Full Scan, Product Ion scan and single ion monitoring mode, referred to as unit resolution. The nebulizer (air) and the curtain gas flows (nitrogen) were set at 10 arbitrary unit (AU). The IonSpray source was operated at 500 °C with the auxiliary gas flow (air) set at 8 L min^{-1}.

First, full scan in positive and negative mode (m/z range 90–500, scan time, declustering potential ±46 V, focussing potential ±190 V) was performed in order to identify the intermediates. Then, product ion scan MS/MS mode (declustering potential ±46 V, focussing potential ±190 V, collision energy 30 eV, precursor ion m/z: 341, 357 and 373) was used for structure elucidation of the main degradation product. As negative ionization mode gave best sensitivity, this polarity ionization mode was retained for reaction kinetic photodegradation determination in single ion monitoring (SIM) (declustering potential −46 V, focussing potential −190 V).

For the HPLC–MS/MS kinetic studies of boscalid photodegradation, aliquots of 300 μL of the reaction mixture were taken at the beginning of the experiment and at regular time intervals during irradiation and after filtration to separate the TiO$_2$ particles.

3. Results and discussion

3.1. Hydrolysis and photolysis

In order to evaluate and compare the efficiency of the photocatalytic process with that of hydrolysis and direct photolysis, preliminary experiments (without the addition of TiO$_2$) were carried out at the same concentration of boscalid ($C_0 = 10.3$ μmol L^{-1} equivalent approximately to 3.5 mg L^{-1}) and initial pH. Fig. 2 illustrates the time course of the concentration of boscalid under three different experimental conditions: (1) in the dark in absence of TiO$_2$ (hydrolysis); (2) UV-irradiation in absence of TiO$_2$ (photolysis); (3) UV-irradiation in presence of TiO$_2$. As expected, irradiation of boscalid in absence of TiO$_2$ showed no significant photodegradation. After 90 min of irradiation, hydrolysis and direct photolysis contributed less than 2% and 8%, respectively, to the degradation process (Fig. 2, curves A and B, respectively) indicating that the photochemical process are scarcely responsible for the observed fast transformation when the solution was irradiated in the presence of TiO$_2$ (Fig. 2, curve D).

3.2. Photocatalytic degradation of boscalid

In the dark with TiO$_2$ (Fig. 2, curve C), a slight decrease of boscalid was observed (9%) after 15 min of continuous stirring due to an adsorption of the pesticide on TiO$_2$ surface.
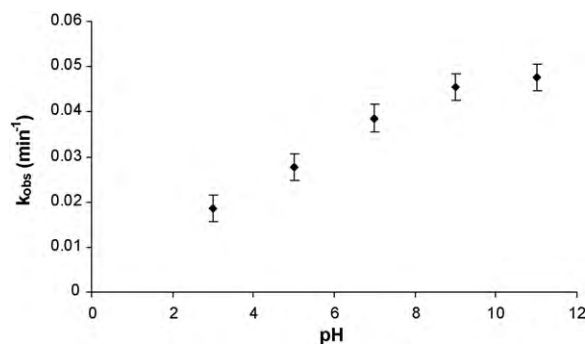

Fig. 3. Effect of pH on degradation kinetics of boscalid.

On the other hand, the complete disappearance of 10.3 μmol L^{-1} solution of boscalid was reached within 90 min (Fig. 2, curve D). Several experimental studies have indicated that the photocatalytical degradation rates of pesticides over illuminated TiO$_2$ could be interpreted by the Langmuir–Hinshelwood (L–H) kinetic model [21–23] but we are aware that the present kinetic data are not sufficient to conclude that the L–H mechanism is the most suitable model to describe the photocatalytic process of boscalid.

As can be seen in the inset in Fig. 2, the logarithm of the ratio of the initial concentration (C_0) to the concentration at a given time (C) versus time (t) is plotted. Boscalid degradation follows a pseudo-first-order kinetic. The value obtained for k_{obs} was 0.35 min^{-1}, determined by calculating the slope of the line. The photocatalysis process was demonstrated to be around 400 times more efficient than boscalid degradation by direct photolysis ($k_{photolysis} = 8.9 \times 10^{-4}$ min^{-1}).

3.2.1. Effect of pH

Many studies have indicated that the pH of a solution is an important parameter in the photocatalytic degradation of organic compounds. This is because the pH determines the surface charge properties of the photocatalyst and therefore the adsorption behaviour of the pollutants [24–27]. Therefore, the influence of pH on the degradation of boscalid in the aqueous suspension of TiO$_2$ was studied at pH ranging from 3 to 11. These initial pH values were adjusted using NaOH or HCl.

Fig. 3 shows the degradation rate for the decomposition of boscalid as a function of reaction pH. The results indicated that the degradation rate decreased with a decrease in pH, and it proceeded much faster under an alkaline pH. The effect of pH on a photocatalytic reaction is generally ascribed to the surface charge of the photocatalyst and its relation to the ionic form of the organic compound (anionic or cationic). Electrostatic attraction or repulsion between the photocatalyst's surface and the organic molecule is taking place, and these events consequently enhance or inhibit, respectively, the photodegradation rate [28,29].

The ionization state of the surface of the photocatalyst can be protonated and deprotonated under acidic and alkaline conditions, respectively, as shown in following equations:

$$TiOH + H^+ \rightarrow TiOH_2^+ \tag{1}$$

$$TiOH + OH^- \rightarrow TiO^- + H_2O \tag{2}$$
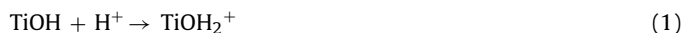
The point of zero charge (pzc) of the TiO$_2$ (Degussa P25) is widely reported at pH ~6.25 [30]. Thus, the TiO$_2$ surface will remain positively charged in acidic medium (pH < 6.25) and negatively charged in alkaline medium (pH > 6.25).

The pH value may also influence the amount of hydroxyl radicals (OH•) formed. OH• can be formed by the reaction between hydroxide ions and light-excited holes (h$^+$) with H$_2$O/OH•. The positive holes are considered as the major oxidation species at low
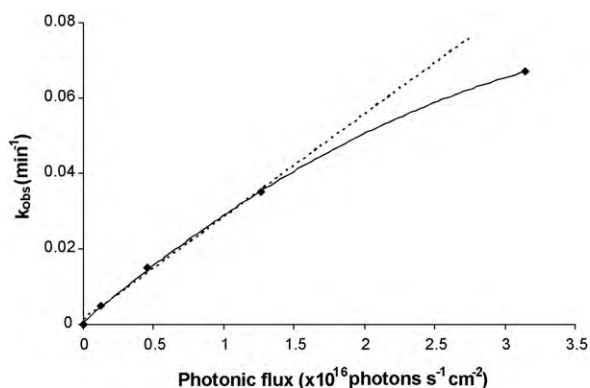
Fig. 4. Influence of the photonic flux on the rate constant of photocatalytic degradation of boscalid.

Table 1
The pseudo-first-order rate constant k_{obs}, half-life $t_{1/2}$, and correlation coefficients for photocatalytic degradation of boscalid at different oxygen concentrations.

$[O_2]$ (mg L^{-1})	k_{obs} (min^{-1})	$t_{1/2}$ (min)	r^2
0	0.0116	59.8	0.986
9	0.0346	20.0	0.993
18	0.0384	18.1	0.992

pH whereas hydroxyl radicals are considered as the predominant species at neutral or high pH levels [31,32].

In this study it has been shown that the degradation for the model compound under investigation is strongly influenced by the reaction pH as shown in Fig. 3. Since boscalid is an unionizable compound, the observed increase of the degradation rate under an alkaline pH can be attributed to the easier generation of OH• by oxidizing more hydroxide ions available on TiO$_2$ surface.

3.2.2. Effect of photonic flux

To investigate the influence of the light flux, this was varied from 0.1 to 3.2×10^{16} photon s^{-1} cm^{-2} and the first-order rate constants of boscalid were measured. The light intensity was regulated by including calibrated grids between the lamp and the reactor. As shown in Fig. 4, different degradation rates were observed when working with different photonic fluxes. The curve obtained shows that for photonic fluxes below 1.3×10^{16} photon s^{-1} cm^{-2}, k_{obs} increases almost linearly, indicating that most of the incident photons are efficiently converted into active species that act in the degradation mechanism. For higher photonic fluxes, the additional photons equally increase the concentration in electrons and holes, which favour their recombination rate which is predominant. This means that the efficiency of the photocatalytic process is limited above 1.3×10^{16} photon s^{-1} cm^{-2}.

### 3.2.3. Oxygen concentration

Considering an important role of oxygen in the photocatalytic degradation of pesticides, several experiments were performed at different oxygen concentrations, 0, 9 and 18 mg L^{-1}, obtained by using as the reaction gas nitrogen, ambient air or oxygen, respectively. As can be seen in Table 1, oxygen concentration has a positive

effect on the degradation process. The rate constant of photocatalytic degradation is higher in the oxygen saturated solution than in deoxygenated solution. On other hand, similar values were obtained for the disappearance of boscalid in the saturated solution and oxygen naturally present in the aerated solution. These results showed that the presence of oxygen observably increased the photocatalytic degradation efficiency of boscalid. Furthermore, the content of oxygen in air is high enough for the degradation of this pesticide since the degradation efficiency in air was similar with that in oxygen. Hence, all the experiments were performed in ambient air.

It is well established that conductive band electrons (e_{CB}^-) and valence band holes (h_{VB}^+) are generated when TiO$_2$ is irradiated with light energy greater than its band gap energy (3.2 eV for anatase) [33,34]:

$$TiO_2 + h\nu \rightarrow h_{VB}^+ + e_{CB}^- \qquad (3)$$

In the illuminated TiO$_2$ system, one practical problem is the undesired electron–hole pair recombination (in the order of nanoseconds), which is the major energy-wasting step and leads to low quantum yield. As Ollis et al. reported [35], oxygen is essential for photocatalytic degradation of organics compounds. Dissolved molecular oxygen is strongly electrophilic and thus its presence reduces unfavourable electron–hole recombination routes by trapping electrons. During this reaction superoxide radical ion ($O_2^{\bullet-}$) which is a reactive species is formed, according to the following reaction:

$$O_2 + e_{CB}^- \rightarrow O_2^{\bullet-} \qquad (4)$$
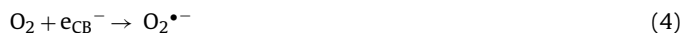
Superoxide radical ions together with hydroxyl radical (•OH) are reported to be responsible for the heterogeneous TiO$_2$ photodecomposition of organic substrates.

3.2.4. Effects of co-existing substances on the degradation of boscalid

The study of the effects of inorganic salts on the photocatalytic degradation of boscalid is important because inorganic species are present in natural water systems. It is interesting to note that these species could enhance boscalid degradation and other species would restrain boscalid degradation by different mechanisms.

It is well known that the photocatalytic reactions occur at the surface of the semiconductor particle so the adsorption of ions may affect the system performance by competing for the oxidizing radicals or blocking the active sites of the TiO$_2$ catalyst. The adsorption degree is dependent on the value of pH and on the exchange reactions with the surface hydroxyl groups. Consequently, the point of zero charge (pzc) should be a determining property degradation.

In this study, the effects of Na$^+$, K$^+$, Ca^{2+} and Mg^{2+} ions on the degradation rate of boscalid were examined individually by adding NaNO$_3$, KNO$_3$, Ca(NO$_3$)$_2$ and Mg(NO$_3$)$_2$ to the system until the resultant solution contained 0.4 M of the cations before the irradiation had begun. According to Table 2, when all the salts were added into aqueous solution, the respective pH values of the solution ranged between 6.3 and 6.7. At these pH values, the TiO$_2$ surface remains negatively charged. The decrease in reaction rate could be due to the adsorption of these cations on TiO$_2$/glass surface. The

Table 2
The pseudo-first-order rate constant k_{obs}, half-life $t_{1/2}$, and correlation coefficients for photocatalytic degradation of boscalid in presence of different cations and anions.

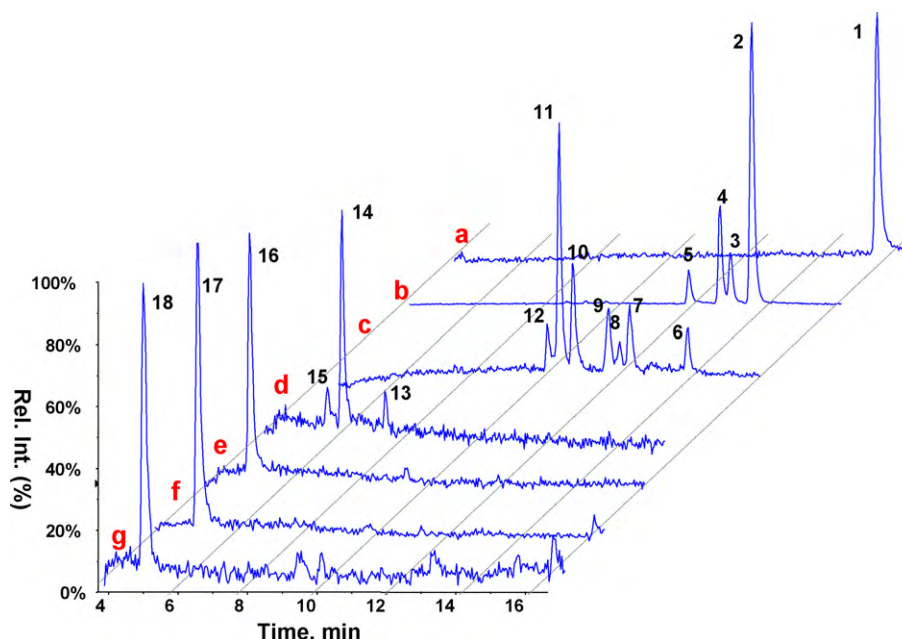| Cations	k_{obs} (min^{-1})	$t_{1/2}$ (min)	r^2	Anions	k_{obs} (min^{-1})	$t_{1/2}$ (min)	r^2
Without cation	0.0346	20.0	0.993	Without anion	0.0346	20.0	0.993
Na$^+$	0.0337	20.6	0.995	Cl$^-$	0.0351	19.8	0.991
K$^+$	0.0325	21.3	0.991	NO$_3^-$	0.0337	20.6	0.995
Ca^{2+}	0.0294	23.6	0.986	SO$_4^{2-}$	0.0352	19.7	0.984
Mg^{2+}	0.0251	27.6	0.990	CO$_3^{2-}$	0.0215	32.2	0.992

Fig. 5. Negative ionspray LC–MS/MS chromatograms of boscalid degradation mixtures: (a) single ion monitoring (SIM) $m/z = 341$ of boscalid, (b) SIM of monohydroxylated boscalid $m/z = 357$, (c) SIM of dihydroxylated boscalid $m/z = 373$, (d) SIM of $m/z = 172$, (e) SIM of $m/z = 156$, (f) SIM of $m/z = 112$ and (g) SIM of $m/z = 224$ (see Table 3 and Fig. 7 for proposed structures).

sequence of inhibition was $Mg^{2+} > Ca^{2+} > K^+ > Na^+$. The effect of Mg^{2+} was the strongest among four cations tested (Table 2). This reveals that the larger the charge and size of cations contained, the more the inhibition of reaction rate increased.

The effects of CO_3^{2-}, SO_4^{2-}, NO_3^- and Cl^- ions on the photodegradation efficiency of boscalid were also investigated by adding Na_2CO_3, Na_2SO_4, $NaNO_3$ and $NaCl$ at 0.4 M. As shown in Table 2, for Cl^-, SO_4^{2-} and NO_3^- no obvious effects on the degradation of boscalid were observed.

The pH values found for these anions were slightly basic in the case of CO_3^{2-}, SO_4^{2-} and similar to pH_{pzc} for Cl^- and NO_3^-. A negligible effect has been already reported by other authors for weakly adsorbed anions such as NO_3^- or SO_4^{2-} [29,36,37]. In the case of Cl^-, Wang et al. [38] indicated that at $pH < pH_{pzc}$, the Cl^- ions are strongly adsorbed on the TiO_2 surface and reduce the photodegradation rate. At neutral or alkaline conditions, the addition of Cl^- ion did not influence the reaction. A second explanation could be that chloride anions, as others halides, are known to scavenge photogenerated holes [39]. They are oxidized by photoholes to chlorine radicals which are reduced back by electrons to chloride ions, hence reducing the availability of holes and electrons. Chlorine radicals can react with organic compounds via addition/elimination reactions (E_0 ($Cl^\bullet/Cl^-$) = 2.5 V). Then these two opposite effects of Cl^- lead in the case of boscalid to an unsignificant effect on its degradation rate.

On the contrary, when CO_3^{2-} was added, the photocatalytic degradation efficiency of boscalid decreased considerably due to the scavenging of hydroxyl free radicals. Radical scavenging could explain why degradation is inhibited by carbonates since these anions are known to strongly scavenge hydroxyl radicals [40]:
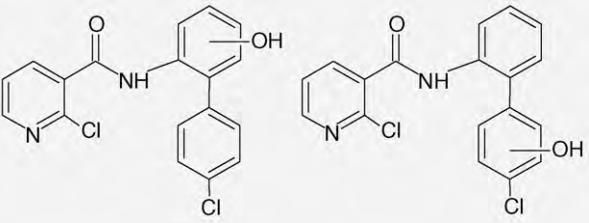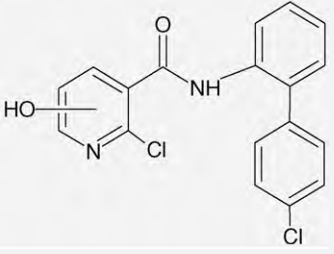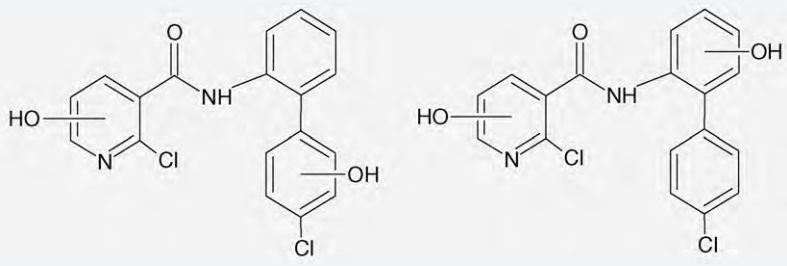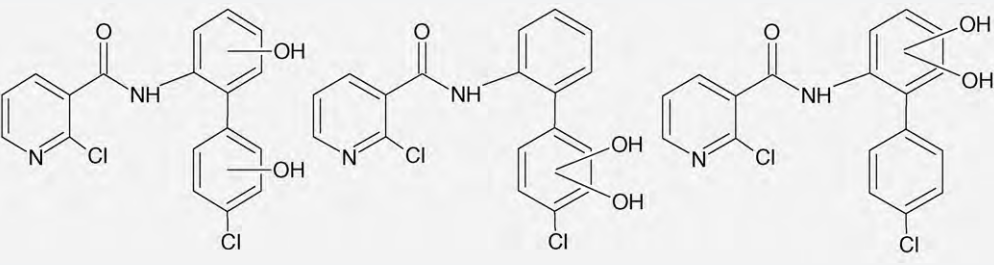
$$CO_3^{2-} + {}^\bullet OH \xrightarrow{k=3.9 \times 10^8 \, L \, mol^{-1} \, s^{-1}} CO_3^{\bullet -} + OH^- \qquad (5)$$
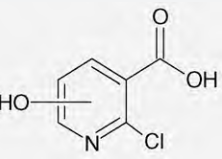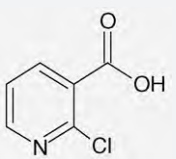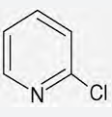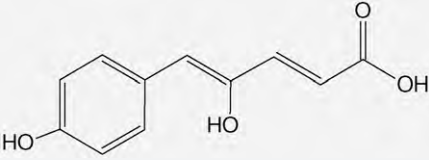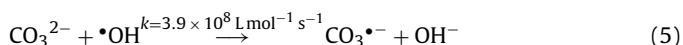
The carbonate radicals that are formed can theoretically react with boscalid. However, they have a lower oxidation potential than hydroxyl radicals (E_0 ($CO_3^{\bullet -}/CO_3^{2-}$) = 1.85 V, E_0 ($OH^\bullet/H_2O$) = 2.80 V), so that their reaction on boscalid is less easy to initiate.

3.3. Identification of the organic intermediates

In order to characterize all the organic intermediates, a mixture of five solutions of boscalid (3.5 mg L^{-1}) irradiated for 15, 30, 60, 90 and 180 min and concentrated by SPE was analyzed by HPLC–MS/MS. This sample represented as much as possible the different intermediates. Blank analysis helped us to discard those peaks coming from the sample handling procedure and chromatographic system. First, molecular weights of photoproducts were determined by Full scan analysis in negative and/or positive ionspray acquisition mode. Then, MS/MS of the major compounds were performed in order to obtain structural information of each photoproduct. Fig. 5 shows the single ion monitoring (SIM) trace in negative ionspray of the boscalid and the 17 major intermediates detected and subsequently identified by interpretation of their MS spectra. These compounds are summarized in Table 3 together with their LC–MS retention times, molecular weights and structure.

As can be seen, compounds **2–5** were identified as monohydroxylated compounds. In order to determine the position of the addition (aromatic or chloropyridine moieties), boscalid mass fragmentation spectra were firstly compared to the photoproducts masses observed during product ion scan analysis. Compounds **2**, **4** and **5** exhibited the same molecular fragment as boscalid ($m/z = 112$) which corresponds to the characteristic loss 2-chloropyridine moiety. Compound **3** exhibited a fragment at ($m/z = 128$). From this observation, it can be concluded that hydroxylation of compound **3** occurred in 2-chloropyridine whereas hydroxylation of compounds **2**, **4** and **5** occurred in aromatics rings. With the same observation, compounds **7–11** were identified as dihydroxylated compounds with both hydroxyls in aromatics ring and compounds **6** and **12**, dihydroxylated compounds with hydroxylation in the aromatic part and in 2-chloro-pyridine moiety. In order to correctly characterise (position of hydroxylation) these compounds, it would be necessary to isolate each hydroxylated compound from the degradation mixture, and to perform its NMR analysis or using an HPLC/^{1}H NMR methods [41] or more simply to determine the most probable positions attacked by a hydroxyl radical with theoretical calculations [42].

Table 3
Mass spectra data and structures of identified intermediates by LC–MS for irradiation boscalid with TiO$_2$.

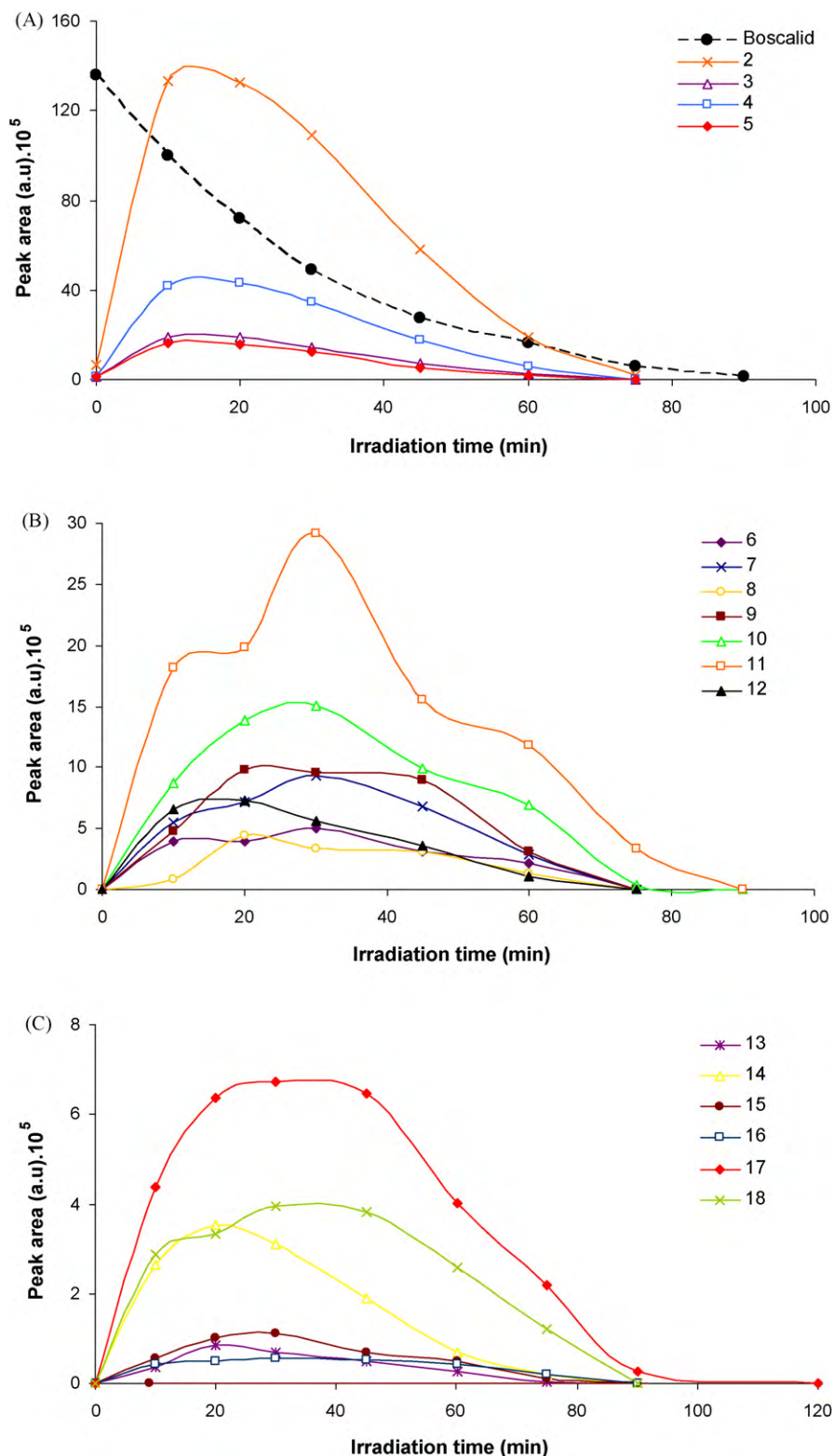| No.	Structure	Retention time (min)	[M−H]$^-$	Negative fragment
2		13.7		
4		12.9	357	112, 244
5		11.8		
3		13.1	357	128, 228
6		13.8	373	
12		9.7		128, 244
7		11.9		
8		11.7		
9		11.5	373	
10		10.0		112, 269
11		9.8		
13		7.3		
14		5.9	172	
15		5.7		
16		5.0	156	
17		5.1	112	
18		5.0	223	

Fig. 6. (A) Evolution of the monohydroxylated products during degradation of boscalid. (B) Evolution of the dihydroxylated products during degradation of boscalid. (C) Evolution of the last intermediates, obtained by the rupture of amide bond, during degradation of boscalid.

3.4. Evolution of intermediates and degradation pathways

In order to better understand the reaction mechanisms involved in the photocatalytic degradation of boscalid, the kinetic evolution of principal intermediates was also followed during the irradiation of a solution of boscalid ($3.5\,mg\,L^{-1}$)

under a photonic flux of $1.3 \times 10^{16}\,photon\,s^{-1}\,cm^{-2}$ (Fig. 6). Thus, aliquots of the reaction mixture were sampled at regular time intervals (10 or 15 min) during photodegradation process up to 360 min and analyzed by HPLC–MS/MS. After 120 min of irradiation, degradation products were not detected.

Fig. 7. Photocatalytic degradation pathway of boscalid.
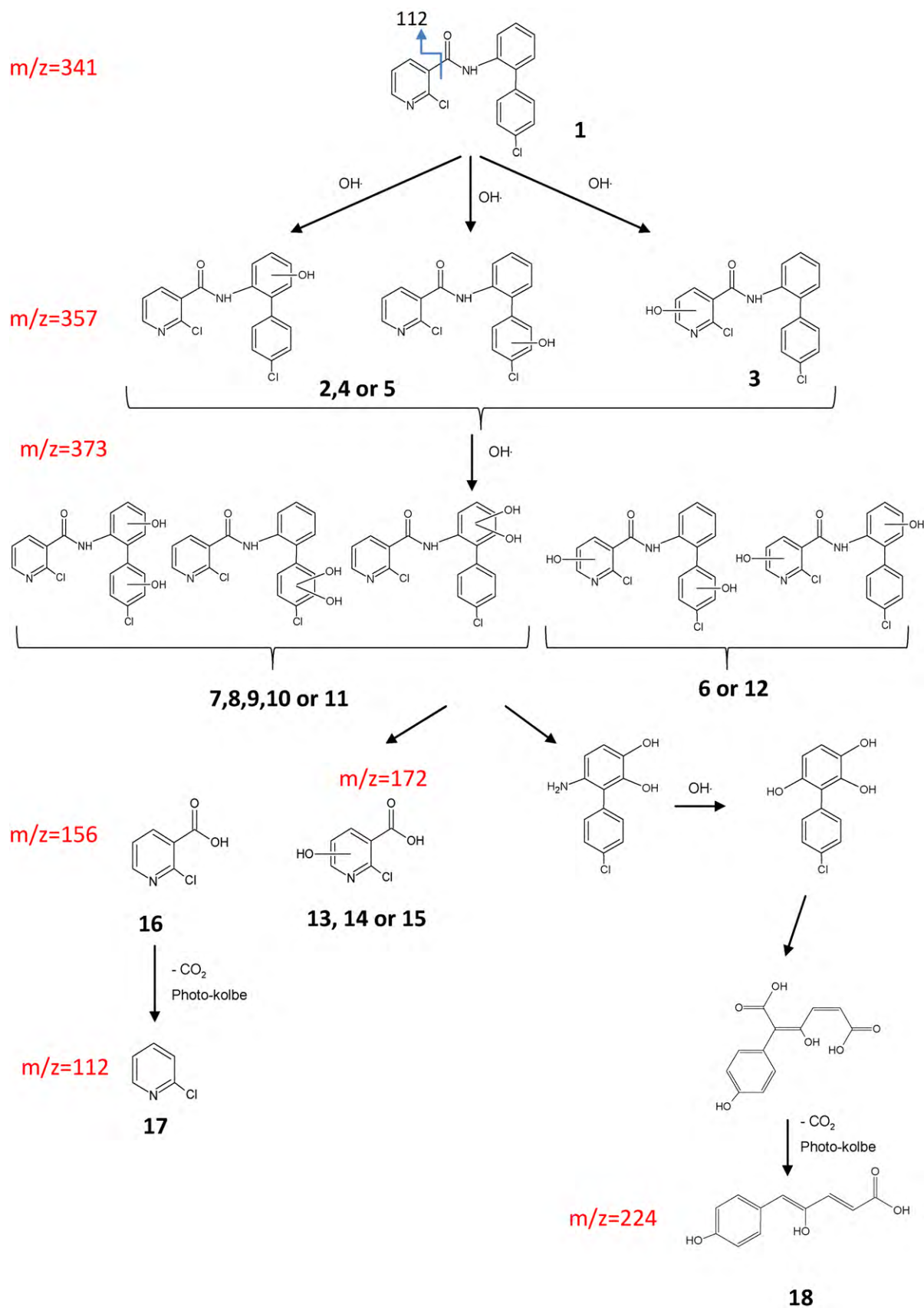
Based on the previous results, a possible photocatalytic degradation pathway of boscalid consisting of several steps was proposed in Fig. 7. As can be seen, all the intermediates are formed in mainly three different ways:

(i) Firstly boscalid is attacked by OH• radicals at −H in the three rings (benzene and pyridine rings) leading to four mono-hydroxylated products **2–5**, which reach their maximum of concentrations around 15 min then decrease progressively to disappear from solution after 70 min, as showed in Fig. 6-a. The products **2**, **4** and **5** are obtained by hydroxylation of the benzene rings whereas the product **3** is obtained by hydroxylation of pyridine. By comparing the evolution profiles for these products it appears that product **2** is the major hydroxylation intermediate whereas products **3–5** are much less important and are formed at very low concentrations, indicating a regioselective attack for the OH• radicals due to the highest electron density of the benzene carbon sites. In addition we can assume (even is HPLC–MS–MS analysis is unable to give us this data) that hydroxyl radicals attack occurs mainly on the carbon in ortho position with respect to chloride atom (product **2**) since it is the most nucleophile.

(ii) The second category of intermediates results from the hydroxylation of the first intermediates (**2–5**) leading to seven dihydroxylated products **6–12**. These products appear at the first minutes of irradiation and their concentration increases to reach a maximum around 30 min (Fig. 6-b). Product **11** is the most abundant whereas **6** and **12** products are the least concentrated which indicates that the OH radicals attack occurs mainly in benzene rings and hydroxylation of pyridine moiety represents only a minor pathway.

(iii) The last intermediates consist of the scission of the amide bond (N–C bond) leading to the formation of compounds **13–18**. As can be seen in Fig. 7, products **13–15** result from the rupture of the amine bond in molecules with the pyridine moiety hydroxylated (**3**, **6** and **12**) and the product **16** from the dyhydroxylated products only in benzene rings (**7–11**). The product **16** is the most abundant (Fig. 6-c) because it was obtained from the principal dihydroxylated products (**10** and **11**) and its decarboxylation leads to product **17**. Moreover, the products dihydroxylated with the two hydroxyl groups in neighbour carbon sites could be transformed in product **18** by the opening of the aromatic ring observed throughout the photocatalysis process [43,44] and a final step of decarboxylation via photokolbe reaction [45].

3.5. Identification and evolution of carboxylic acids

Carboxylic acids formed during the degradation process of the 10.3 μmol L^{-1} boscalid solution were identified by HPLC-UV. Therefore, irradiated samples of boscalid were analyzed. Five major acids were identified (oxalic, formic, acetic, malonic and glyoxylic) by comparison with commercial standards. They are formed since the beginning of photodegradation. Malonic acid is the first and the major one. Its concentration increases to reach at 45 min a value of 21.5 μmol L^{-1}. Acetic acid is the second one. It appears after 15 min of irradiation and is accumulated up to 19.4 μmol L^{-1} and hence, it is slowly destroyed to approximately 2 μmol L^{-1} at 360 min. Glyoxylic and oxalic acids reached their maximum concentration of 14.2 and 8.5 μmol L^{-1} after 120 and 90 min of UV-irradiation, respectively, and then diminished slowly. Brillas and Oturan [46] have demonstrated that glyoxylic acid was transformed into oxalic acid. The oxalic disappearance between 100 and 300 min is related to its direct transformation into two molecules of CO$_2$. Formic acid
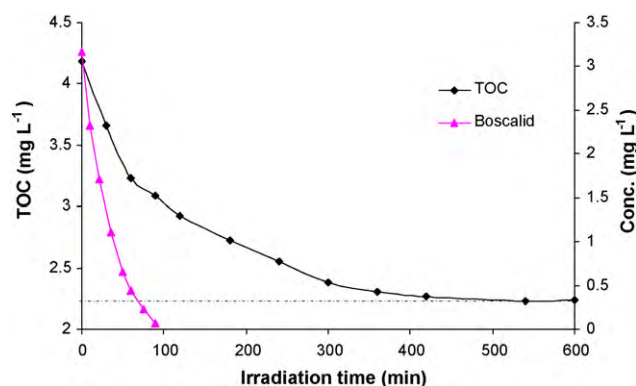

Fig. 8. Total organic carbon (TOC) removal during boscalid photocatalysis.

appears after 120 min resulting mainly from the transformation of acetic acid, and disappears from the solution by transformation into CO$_2$.

3.6. Mineralization

Complete mineralization is very important for organic pollutants photocatalysis. The breaking down of the benzene ring and subsequent mineralization leading to water and carbon dioxide could be visualized by the decrease in TOC during the photocatalytic process. To assess the extent of mineralization during the photocatalytic degradation of boscalid, TOC was monitored as shown in Fig. 8. It showed TOC removal followed a much slower rate compared to degradation of boscalid. The mineralization kinetic is rapid at the two first hours of the treatment but becomes much slower at longer time because carboxylic acids formed by oxidative ring opening reactions are less reactive toward hydroxyl radicals compared to the aromatics. Thus, they are degraded more slowly than the pesticide initially introduced. Complete TOC removal was achieved after long irradiation time (around 400 min) to reach a constant number equal to 2.2, which corresponds to the measure of TOC for TiO$_2$ aqueous solution (background noise).

4. Conclusions

Photodegradation using TiO$_2$ as a catalyst is an efficient method for degrading boscalid. At optimal operating parameters, a complete degradation was achieved after 90 min irradiation. On kinetic study, degradation rate of boscalid followed a pseudo-first-order kinetic, suggesting an associative adsorption of the molecule on the TiO$_2$ surface. The photodegradation rate was found to increase along with increasing pH, photonic flux and oxygen concentration. In addition, the presence of inorganic cations such as Na$^+$, K$^+$, Ca^{2+} and Mg^{2+} and anions as CO$_3$$^{2-}$ that are often presented in natural water systems decreased the photocatalytic degradation rate of boscalid.

Seventeen intermediates have been identified and characterized through a mass spectra analysis using HPLC–MS/MS, giving insight into the early steps of the degradation process. The evolution of these intermediates and TOC, allowed a better understanding of the degradation mechanism. The pathway proposed consists of three main competitive pathways: the monohydroxylation of boscalid in benzene and pyridine rings, the dihydroxylation of these first products and the rupture of the N–C bond followed by decarboxylation via photokolbe reaction. Finally, aromatic rings opening leads to the formation of carboxylic acids such as oxalic, formic, acetic, malonic and glyoxylic.

Acknowledgements

References

[1] E. Charizopoulos, E. Papadopoulou-Mourkidou, Environ. Sci. Technol. 33 (1999) 2363–2368.
[2] S.P. Hatzilazarou, E.T. Charizopoulos, E. Papadopoulou-Mourkidou, A.S. Economou, Pest Manage. Sci. 60 (2004) 1197–1204.
[3] A. Papastergiou, E. Papadopoulou-Mourkidou, Environ. Sci. Technol. 35 (2001) 63–69.
[4] D.W. Kolpin, J.E. Barbash, R.J. Gillom, Environ. Sci. Technol. 32 (1998) 558–566.
[5] L. Fang, Chin. J. Appl. Ecol. 11 (2000) 249–252.
[6] A.K. Hall, J.M. Harrowfield, R.J. Hart, P.G. Mccormick, Environ. Sci. Technol. 30 (1996) 3401–3407.
[7] M. Kim, P.W. Okeefe, Chemosphere 41 (2000) 793–800.
[8] G.H. Liu, Y.F. Zhu, X.R. Zhang, B.Q. Xu, Anal. Chem. 74 (2002) 6279–6284.
[9] W. Choi, S.J. Hong, Y.S. Chang, Y. Cho, Environ. Sci. Technol. 34 (2000) 4810–4815.
[10] L. Zan, W.J. Fa, S.L. Wang, Environ. Sci. Technol. 40 (2006) 1681–1685.
[11] S. Malato, J. Blanco, C. Richter, B. Milow, M.I. Maldonado, Water Sci. Technol. 40 (1999) 123–130.
[12] S. Malato, J. Blanco, A. Vidal, C. Richter, Appl. Catal. B 37 (2002) 1–15.
[13] K. Nagaveni, G. Sivalingam, M.S. Hegde, G. Madras, Appl. Catal. B: Environ. 48 (2004) 83–93.
[14] S.C. Panchangam, A.Y.-C. Lin, K.L. Shaik, C.-F. Lin., Chemosphere 77 (2009) 242–248.
[15] G.R.M. Echavia, F. Matzusawa, N. Negishi, Chemosphere 76 (2009) 595–600.
[16] S. Liu, M. Lim, R. Fabris, C. Chow, M. Drikas, R. Amal, Environ. Sci. Technol. 42 (2008) 6218–6223.
[17] P. Calza, V.A. Sakkas, C. Medana, C. Baiocchi, A. Dimou, E. Pelizzetti, T. Albanis, Appl. Catal. B: Environ. 67 (2006) 197–205.
[18] I.K. Konstantinou, T.A. Albanis, Appl. Catal. B: Environ 49 (2004) 1–14.
[19] C.G. Da Silva, J.L. Faria, J. Photochem. Photobiol. A: Chem. 155 (2003) 133–143.
[20] N. Daneshvar, D. Salari, A.R. Khataee, J. Photochem. Photobiol. A: Chem. 157 (2003) 111–116.
[21] J.C. D'Oliveria, G. Al-Sayyed, P. Pichat, Environ. Sci. Technol. 24 (1990) 990–996.
[22] C.S. Rurchi, D.R. Ollis, J. Catal. 122 (1990) 178–192.
[23] J.M. Herrmann, Top. Catal. 34 (2005) 49–65.
[24] J. Matos, A. Garcia, T. Cordero, J.M. Chovelon, C. Ferronato, Catal. Lett. 130 (2009) 568–574.
[25] U.G. Akpan, B.H. Hameed, J. Hazard. Mater. 170 (2009) 520–529.
[26] X. Zhu, C. Yuan, Y. Bao, J. Yang, Y. Wu, J. Mol. Catal. A 229 (2005) 95–105.
[27] C. Fernández, M. Soledad Larrechia, M. Pilar Callao, Talanta 79 (2009) 1292–1297.
[28] C.S. Lua, C.C. Chenb, F.D.H. Maic, K. Li, J. Hazard. Mater. 165 (2009) 306–316.
[29] L. Wei, Ch. Shifu, Z. Wei, Z. Sujuan, J. Hazard. Mater. 164 (2009) 154–160.
[30] C. Kormann, D.W. Bahnemann, M.R. Hoffmann, Environ. Sci. Technol. 25 (1991) 494–500.
[31] W.Z. Tang, C.P. Huang, Water Res. 29 (1995) 745–756.
[32] S. Tunesi, M. Anderson, J. Phys. Chem. 95 (1991) 3399–3405.
[33] I.K. Kongstantinou, T.M. Sakellarides, V.A. Sakkas, T.A. Albanis, Environ. Sci. Technol. 35 (2001) 398–405.
[34] W. Choi, M.R. Hoffmann, Environ. Sci. Technol. 29 (1995) 1646–1654.
[35] D.F. Ollis, E. Pelizzetti, N. Serpone, Environ. Sci. Technol. 25 (1991) 1522–1529.
[36] M. Abdullah, J.K.C. Low, R.W. Matthews, J. Phys. Chem. 94 (1990) 6820–6825.
[37] J.C. D'Oliveira, C. Guillard, C. Maillard, P. Pichat, J. Environ. Sci. Health A 28 (1993) 941–956.
[38] K.H. Wang, Y.H. Hsieh, C.H. Wu, C.Y. Chang, Chemosphere 40 (2000) 389–394.
[39] P. Calza, E. Pelizzetti, Pure Appl. Chem. 73 (2001) 1839–1848.
[40] A. Lair, C. Ferronato, J.M. Chovelon, J.M. Herrmann, J. Photochem. Photobiol. A: Chem. 193 (2008) 193–203.
[41] M. Sleiman, P. Conchon, C. Ferronato, J.M. Chovelon, Appl. Catal. B: Environ. 71 (2007) 279–290.
[42] A. Piram, R. Faure, H. Chermette, C. Bordes, B. Herbreteau, A. Salvador, J. Environ. Anal. Chem., accepted, doi:10.1080/03067319.2010.497920.
[43] R. Matthews, J. Catal. 111 (1998) 264–272.
[44] S. Chatterjee, S. Sarkar, S.N. Bhattacharyya, J. Photochem. Photobiol. A: Chem. 81 (1994) 199–203.
[45] B. Krautler, A.J. Bard, J. Am. Chem. Soc. 10 (1978) 2239–2245.
[46] E. Brillas, M.A. Oturan, Pesticides: Impacts Environnementaux, in: M.A. Oturan, J.M. Mouchel (Eds.), Gestion et Traitements, 2007, pp. 61–73 (Chapitre 2).